



UNIVERSITY  
OF WOLLONGONG  
AUSTRALIA

University of Wollongong  
Research Online

---

Faculty of Engineering and Information Sciences -  
Papers: Part A

Faculty of Engineering and Information Sciences

---

2015

# Attenuation and propagation of voltage unbalance in radial distribution networks

Devinda Perera

*University of Wollongong, bmdp065@uowmail.edu.au*

Philip Ciufu

*University of Wollongong, ciufu@uow.edu.au*

Lasantha G. Meegahapola

*Royal Melbourne Institute of Technology, lasantha.meegahapola@rmit.edu.au*

Sarath Perera

*University of Wollongong, sarath@uow.edu.au*

---

## Publication Details

D. Perera, P. Ciufu, L. Meegahapola & S. Perera, "Attenuation and propagation of voltage unbalance in radial distribution networks," *International Transactions on Electrical Energy System*, vol. 25, (12) pp. 3738-3752, 2015.

Research Online is the open access institutional repository for the University of Wollongong. For further information contact the UOW Library:  
[research-pubs@uow.edu.au](mailto:research-pubs@uow.edu.au)

---

# Attenuation and propagation of voltage unbalance in radial distribution networks

## **Abstract**

Recently published International Electrotechnical Committee (IEC) technical reports IEC 61000-3-13 provides detailed methodologies for managing voltage unbalance (VU) in electric power systems. A key aspect in the VU emission allocation process is the estimation of VU propagation in different parts of the network. Although the VU propagation from upstream networks to downstream networks is adequately addressed, the attenuation of VU when propagating from downstream to upstream networks at the same voltage level has not been properly taken into account in the aforementioned methodologies. Furthermore, mains connected three-phase induction motors are known to attenuate VU, and there is no methodology currently available to quantify the attenuation provided by such motors. The main motivation behind the current research is to investigate the VU propagation and attenuation in radial distribution networks and to quantify the attenuation provided by induction motor loads. This paper reports that the VU propagation from downstream to upstream in a radial distribution network with symmetrical distribution lines can be conservatively approximated by the ratio of fault levels of upstream and downstream network. Moreover, an influence coefficient has been introduced as a means of appraising the impact of induction motor loads. The theoretical work presented is verified using unbalanced load flow analysis. The outcomes presented in the paper are useful for the further development of IEC technical report on VU emission allocation.

## **Keywords**

propagation, attenuation, networks, unbalance, distribution, voltage, radial

## **Disciplines**

Engineering | Science and Technology Studies

## **Publication Details**

D. Perera, P. Ciufo, L. Meegahapola & S. Perera, "Attenuation and propagation of voltage unbalance in radial distribution networks," *International Transactions on Electrical Energy System*, vol. 25, (12) pp. 3738-3752, 2015.

# Attenuation and Propagation of Voltage Unbalance in Radial Distribution Networks

D. Perera, P. Ciufu, L. Meegahapola and S. Perera,

## Abstract

Recently published International Electrotechnical Committee (IEC) technical reports IEC 61000-3-13 provides detailed methodologies for managing voltage unbalance (VU) in electric power systems. A key aspect in the VU emission allocation process is the estimation of VU propagation in different parts of the network. Although the VU propagation from upstream networks to downstream networks is adequately addressed, the attenuation of VU when propagating from downstream to upstream networks at the same voltage level has not been properly taken into account in the aforementioned methodologies. Furthermore, mains connected three-phase induction motors are known to attenuate VU and there is no methodology currently available to quantify the attenuation provided by such motors. The main motivation behind the current research is to investigate the VU propagation and attenuation in radial distribution networks and to quantify the attenuation provided by induction motor loads. This paper reports that the VU propagation from downstream to upstream in a radial distribution network with symmetrical distribution lines, can be conservatively approximated by the ratio of fault levels of upstream and downstream network. Moreover, an influence coefficient has been introduced as a means of appraising the impact of induction motor loads. The theoretical work presented is verified using unbalanced load flow analysis. The outcomes presented in the paper are useful for the further development of IEC technical report on VU emission allocation.

## Index Terms

emission allocation, radial power systems, three-phase induction motors, voltage unbalance, voltage unbalance attenuation, voltage unbalance transfer coefficient

## I. INTRODUCTION

The International Electrotechnical Vocabulary (IEV 161-08-09) defines voltage unbalance (VU) as a condition in poly-phase electric power systems in which the magnitudes of the fundamental phase voltages and/or the associated phase angles of separation are not equal. The presence of excessive levels of VU stands as a problem of power quality that has far reaching consequences for both customers and electric utilities [1], [2].

Although unbalance arises as a result of unbalanced installations and other, inherent system asymmetries, determining the level of contributions to the total VU emission at the point of connection of a plant is not a straightforward procedure. There are complex interactions that can take place between numerous sources, particularly in an interconnected network environment [3].

IEC technical report IEC 61000-3-13 [4] has been developed in order to provide guidelines and recommendations for managing VU emission in electric power systems. An integral part of the proposed methodologies is the assessment of VU propagation and attenuation [5].

VU, when propagating from an upstream network to a downstream network (i.e. HV to MV) has been studied in [6]–[8]. It is shown that the VU transfer coefficient, which relates the

D. Perera, P. Ciufu, and S. Perera are with the School of Electrical, Computer and Telecommunications Engineering, University of Wollongong, and are Members of the Endeavour Energy Power Quality and Reliability Centre, NSW 2522, Australia (email: ciufu@uow.edu.au).

L. Meegahapola is with the School of Electrical and Computer Engineering at the Royal Melbourne Institute of Technology, Melbourne, Australia

Please address all correspondence to Dr Phil Ciufu, ciufu@uow.edu.au

VU attenuation when it propagates from the upstream network (e.g. transformer HV terminal) to a point of interest (POI) at the downstream network (e.g. transformer MV terminal), to be dependent on load composition further downstream to the POI. In the presence of constant power loads in the network downstream to the POI, VU would magnify at the POI, whereas when induction motor loads are present the VU at the POI would attenuate [8].

VU will also attenuate when propagating from a downstream network to an upstream network. This is particularly important in the emission allocation process where VU attenuation when propagating from downstream to upstream at the same voltage level has to be taken into consideration in order to utilise the network VU absorption capacity to the full extent. Although the recent research on VU emission assessment [9] has established a generalised methodology which can be used to quantify the VU propagation, the proposed methodologies require significant amounts of data, which are not readily available. The VU attenuation characteristics of mains connected three-phase induction motors are widely known in established literature [6], [8]–[10]. The authors of [9], consider an induction motor and an unbalanced passive load connected to the same point of connection (PCC), where it is shown that the VU at the PCC has improved due to the presence of the induction motor load. However, the influence of such motor loads on VU at the PCC of an unbalanced load, when both loads are connected to two separate PCCs of the same network is not established.

The motivation of the current research is to investigate the VU attenuation in radial distribution networks in general and to propose a methodology to estimate the VU in radial distribution networks using readily available data. In addition, a new methodology to quantify the attenuation provided by the three-phase induction motor, when an induction motor and an unbalanced load are connected to two different PCCs of the same distribution network is presented. All simulation studies are conducted on a three-wire, 12.47 kV radial distribution network.

The remainder of the paper is structured as follows. In Section II, VU propagation in radial distribution networks is investigated in for radial distribution networks by employing mathematical models, which are then verified using unbalanced load-flow analysis. Section III examines the VU attenuation and propagation when multiple unbalanced loads are connected to a radial network. Section IV propose a generalised methodology, which can be used to estimate VU in a radial distribution network, where multiple unbalanced installations are connected. The impacts of induction motors on VU emission and propagation are analysed in Section IV. Conclusions are given in Section V.

## II. DEPENDENCY OF VOLTAGE UNBALANCE TRANSFER COEFFICIENT ON FAULT LEVEL

Consider the radial HV/MV distribution network shown in Fig. 1. The two busbars  $j$  and  $k$  respectively are connected downstream to the MV busbar. The purpose is to assess the VU at these two busbars which is caused by the asymmetrical load connected at the  $j^{\text{th}}$  busbar, while the voltage at the upstream HV busbar is considered to be balanced. In order to develop a generic expression for VU at each busbar, the HV/MV transformer and the distribution line sections  $MV - j$  and  $j - k$  are assumed to be asymmetrical. The notations used in Fig. 1 are explained as follows.

$Z_{11:HV-MV}$ ,  $Z_{22:HV-MV}$  - positive-sequence and negative-sequence impedance of the HV/MV transformer respectively

$Z_{11:MV-j}$ ,  $Z_{22:MV-j}$  - positive-sequence and negative-sequence impedance of the distribution line between the MV busbar and  $j^{\text{th}}$  busbar respectively

$Z_{11:j-k}$ ,  $Z_{22:j-k}$  - positive-sequence and negative-sequence impedance of the distribution line between the  $j^{\text{th}}$  busbar and  $k^{\text{th}}$  busbar respectively

$Z_{11:HV-j}$ ,  $Z_{22:HV-j}$  - positive-sequence and negative-sequence impedance of the system

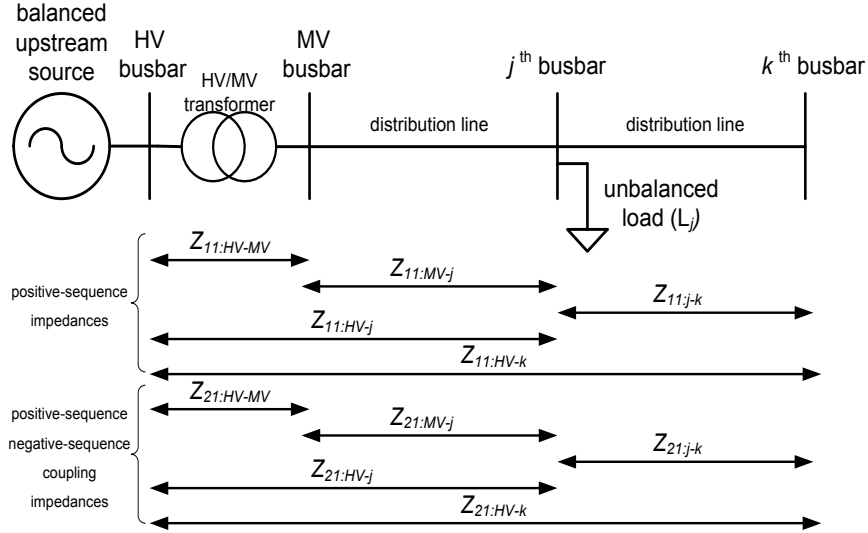


Fig. 1. Radial distribution network

between the HV busbar and  $j^{\text{th}}$  busbar respectively

$Z_{11:HV-k}$ ,  $Z_{22:HV-k}$  - positive-sequence and negative-sequence impedance of the system between the HV busbar and  $k^{\text{th}}$  busbar respectively

$Z_{21:HV-MV}$  - negative-sequence positive-sequence coupling impedance<sup>1</sup> of the HV/MV transformer (generally equals to zero)

$Z_{21:HV-j}$  - negative-sequence positive-sequence coupling impedance of the system between the HV busbar and the  $j^{\text{th}}$  busbar

Referring to Fig. 1 and detailed derivations given in Appendix A, the positive-sequence voltages and negative-sequence voltages at the HV busbar, MV busbar and  $j^{\text{th}}$  busbar are given in (1)-(4):

$$U_{1:HV} = Z_{11:HV-MV} \cdot I_{1:L_j} + U_{1:MV} \quad (1)$$

$$U_{1:HV} = Z_{11:HV-j} \cdot I_{1:L_j} + U_{1:j} \quad (2)$$

$$U_{2:HV} = Z_{22:HV-MV} \cdot I_{2:L_j} + Z_{21:HV-MV} \cdot I_{1:L_j} + U_{2:MV} \quad (3)$$

$$U_{2:HV} = Z_{22:HV-j} \cdot I_{2:L_j} + Z_{21:HV-j} \cdot I_{1:L_j} + U_{2:j} \quad (4)$$

where;

$U_{1:HV}$ ,  $U_{2:HV}$  - positive-sequence and negative-sequence voltages at the HV busbar respectively

$U_{1:MV}$ ,  $U_{2:MV}$  - positive-sequence and negative-sequence voltages at the MV busbar respectively

$U_{1:j}$ ,  $U_{2:j}$  - positive-sequence and negative-sequence voltages at the  $j^{\text{th}}$  busbar respectively

$I_{1:L_j}$  and  $I_{2:L_j}$  are positive-sequence and negative-sequence currents of the load which is

connected at the  $j^{\text{th}}$  busbar respectively

Furthermore, the positive-sequence load current  $I_{1:L_j}$  can be given by (5):

$$I_{1:L_j} = \frac{U_{1:j}}{Z_{11:L_j}} \quad (5)$$

The negative-sequence current of the load  $I_{2:L_j}$  can be expressed in terms of the current unbalance factor<sup>2</sup> (CUF) of the load as (6):

$$I_{2:L_j} = CUF_{L_j} \cdot \frac{U_{1:j}}{Z_{11:L_j}} \quad (6)$$

where  $CUF_{L_j}$  and  $Z_{11:L_j}$  are the current unbalance factor (CUF) and the positive-sequence impedance of the load which is connected at the  $j^{\text{th}}$  busbar respectively.

Employing the fact that the negative-sequence impedance associated with distribution lines, transformers and passive loads are equal to the corresponding positive-sequence impedance, the negative-sequence impedance terms in (3) and (4) can be replaced by their corresponding positive-sequence impedance terms. Substituting the  $I_{1:L_j}$  and  $I_{2:L_j}$  given by (5) and (6) respectively, in (1)-(4), and considering the fact that the voltage at the sending end busbar is balanced (i.e.  $U_{2:HV} = 0$ ), the voltage unbalance factor<sup>3</sup> (VUF) at the  $j^{\text{th}}$  busbar ( $VUF_j$ ) can be expressed as (7):

$$VUF_{L_j} = -\left(\frac{Z_{11:HV-j}}{Z_{11:L_j}} \cdot CUF_{L_j} + \frac{Z_{21:HV-j}}{Z_{11:L_j}}\right) \quad (7)$$

Similarly, the VUF at the MV busbar ( $VUF_{MV}$ ) can be obtained as (8):

$$VUF_{MV} = -\left(\frac{Z_{11:HV-MV}}{Z_{11:L_j}} \cdot CUF_{L_j} + \frac{Z_{21:HV-MV}}{Z_{11:L_j}}\right) \cdot \frac{Z_{11:L_j}}{Z_{11:HV-MV} + Z_{11:L_j}} \quad (8)$$

The term  $\frac{Z_{11:L_j}}{Z_{11:HV-MV} + Z_{11:L_j}}$  in (8) can be re-written in-terms of the positive-sequence voltage at the the MV busbar and  $j^{\text{th}}$  busbar as,  $\frac{U_{1:j}}{U_{1:HV}}$ . Hence,  $VUF_{MV}$  can be re-expressed as (9):

$$VUF_{MV} = -\left(\frac{Z_{11:HV-MV}}{Z_{11:L_j}} \cdot CUF_{L_j} + \frac{Z_{21:HV-MV}}{Z_{11:L_j}}\right) \cdot \frac{U_{1:j}}{U_{1:HV}} \quad (9)$$

The VU transfer coefficient from the  $j^{\text{th}}$  busbar to MV busbar  $T_{u:j-MV}$ , is defined as the ratio of VUF of the MV busbar ( $VUF_{MV}$ ) to VUF of the  $j^{\text{th}}$  busbar ( $VUF_j$ ). Hence,  $T_{u:j-MV}$  can be expressed as (10):

$$T_{u:j-MV} = \frac{Z_{11:HV-MV} \cdot CUF_{L_j} + Z_{21:HV-MV}}{Z_{11:HV-j} \cdot CUF_{L_j} + Z_{21:HV-j}} \cdot \frac{U_{1:j}}{U_{1:HV}} \quad (10)$$

Generally, for three-phase transformers and symmetrical distribution lines the associated negative-sequence positive-sequence coupling impedance is zero. Hence, the terms  $Z_{21:HV-MV}$  and  $Z_{21:HV-j}$  in (10) can be disregarded. Furthermore, assuming that  $U_{1:j} \approx U_{1:HV}$ , (10) can be expressed as (11):

<sup>1</sup>When distribution lines and transformers are asymmetrical, unequal mutual impedance between individual phases cause unbalanced voltages across three phases. Presence of these unequal mutual impedance result in off diagonal elements in the sequence domain impedance matrix.  $Z_{21}$  in the sequence domain is identified as the negative-sequence positive-sequence coupling impedance [12].

<sup>2</sup>The CUF is defined as the ratio of negative-sequence current to positive-sequence current of the load [4]

<sup>3</sup>The VUF is defined as the ratio of negative-sequence voltage to positive-sequence voltage [13]

$$T_{u:j-MV} \approx \frac{Z_{11:HV-MV}}{Z_{11:HV-j}} \quad (11)$$

Equation (11) implies that the transfer of VUF due to the asymmetry of a load from the  $j^{\text{th}}$  busbar to MV busbar can be approximated by the ratio of positive-sequence Thévenin impedance of the MV busbar and  $j^{\text{th}}$  busbar; hence, related to short-circuit capacity of each busbar. The magnitude of transfer coefficient can be evaluated using (12):

$$|T_{u:j-MV}| \approx \left| \frac{S_{sc:j}}{S_{sc:MV}} \right| \quad (12)$$

where;  $S_{sc:MV} = \frac{V_n^2}{Z_{11:HV-MV}}$  is the short-circuit capacity (in MVA) at the MV busbar,  $S_{sc:j} = \frac{V_n^2}{Z_{11:HV-j}}$  is the short-circuit capacity (in MVA) at the  $j^{\text{th}}$  busbar and  $V_n$  is nominal line to line voltage of the network.

Equations (11) and (12) are independent of the load impedance, hence, they can facilitate evaluation of the VU transfer coefficient irrespective of the type of load connected (i.e. constant impedance, constant power etc.) at the  $j^{\text{th}}$  busbar. As the  $k^{\text{th}}$  busbar is unloaded, VUF at the  $k^{\text{th}}$  busbar is equal to the VUF at the  $j^{\text{th}}$  busbar; hence, VU transfer coefficient from  $j^{\text{th}}$  busbar to  $k^{\text{th}}$  busbar is equal to unity.

### III. VALIDATION OF VOLTAGE UNBALANCE TRANSFER MODEL

In order to validate the mathematical formulation of the downstream to upstream VU transfer given in Section II, a 12.47 kV distribution network similar to Fig. 1 is utilised. The 138/12.47 kV HV/MV transformer is assumed to be symmetrical. An asymmetrical load, with per-phase capacity of 4 MVA and lagging power factors of 0.6, 0.7 and 0.8 in phases A, B and C respectively is connected at the  $j^{\text{th}}$  busbar. The distribution line which connects the  $j^{\text{th}}$  busbar to the MV busbar has length of 1.6 km. The distribution network was modelled as a three-wire network using the phase impedance matrix given in Appendix B.

The VU transfer coefficients are evaluated using (10) and (11) for the following four different cases.

- Case 1: The distribution line is symmetrical (i.e.  $Z_{21:MV-j} = 0$ ) and the load is of constant impedance type
- Case 2: The distribution line is symmetrical and the load is of constant power type.

The loads were modelled as constant impedance and constant power loads using voltage dependency model. The unbalance load flow studies were conducted using DIgSILENT Power Factory software, and were solved using Newton Raphson method. The sequence voltage components are computed for each busbar in the network from the unbalanced load flow results and a separate calculation is then used in order to calculate the VU transfer coefficients

The resulting VU transfer coefficient from the  $j^{\text{th}}$  busbar to the MV busbar ( $T_{u:j-MV}$ ) obtained using unbalanced load-flow analysis are compared against results from (12), and are presented in Table I.

According to the results presented in Table I, the VU transfer coefficients  $T_{u:j-MV}$  established using the proposed formulation are seen to be in close agreement with the values given by unbalanced load-flow analysis. In the case of a balanced distribution line, the estimated VU transfer coefficient derived from (12) shows a minor discrepancy compared with the load-flow results. This discrepancy arises due to the approximations made in the derivation of (12).

TABLE I  
COMPARISON OF VU TRANSFER COEFFICIENT BETWEEN THE  $j^{\text{th}}$  BUSBAR AND THE MV BUSBAR ( $T_{u:j-MV}$ )  
ESTABLISHED USING THE MATHEMATICAL MODEL AND LOAD-FLOW ANALYSIS.

	Case 1	Case 2
Load-flow analysis	0.51∠0.17	0.50∠0.17
Equation (10)	0.51∠0.17	0.50∠0.17
Equation (11)	0.53	0.53

Fig. 2 illustrates the cumulative distribution function of  $T_{u:j-MV}$  for the test network when a load-flow analysis was conducted for 5000 cases, where the per-phase capacities of the load are randomly varied and the distribution line is considered to be fixed and symmetrical. (MVA capacities of each phase of the load were generated using a normally distributed random variable, with means of 3.40 MW and 2.12 MVar and standard deviation of 0.26 MW and 0.16 MVar)<sup>4</sup>.  $T_{u:j-MV}$  can be seen to remain approximately constant at 0.51 for constant impedance loads and at 0.505 for constant power loads irrespective of the random variation of per phase capacities of the load. These values are slightly smaller than 0.53 estimated using (12); hence, (12) provides a conservative approximation for downstream to upstream VU propagation.

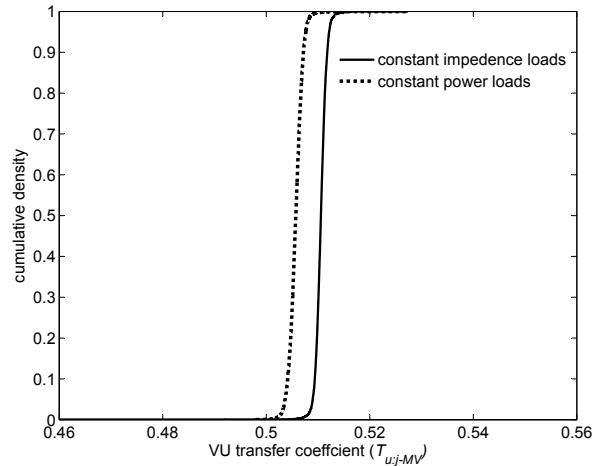


Fig. 2. Cumulative distribution function of downstream to upstream VUF transfer coefficient for constant impedance and constant power loads for the case of fixed symmetrical line.

#### IV. ANALYSIS OF MULTIPLE UNBALANCED LOADS

In order to investigate the VU emission and propagation when multiple loads are connected to a radial distribution network, the radial network shown in Fig. 1 is modified by connecting an additional unbalanced passive load to the  $k^{\text{th}}$  busbar. Both distribution line sections are assumed to be symmetrical. Table II provides the resulting expressions for total VUF at the

<sup>4</sup>The mean and standard deviation of a load's active and reactive power are selected such that the power factor of each phase is within the typical values for an industrial customer for all cases.



TABLE II  
VUFs AT THE  $j^{\text{th}}$  BUSBAR AND  $k^{\text{th}}$  WHEN BOTH LOADS ARE OPERATING SIMULTANEOUSLY.

$VUF_{MV:\text{net}}$	$VUF_{j:\text{net}}$	$VUF_{k:\text{net}}$
$\frac{Z_{11:HV-MV} + \frac{Z_{11:HV-MV} \cdot Z_{11:HV-k}}{Z_{11:j-k}}}{\frac{Z_{11:HV-j}}{Z_{11:L_j}} + \frac{Z_{11:HV-j}}{Z_{11:j-k} + Z_{11:L_k}}} \cdot VUF_{j:\text{net}} +$ $\frac{\frac{Z_{11:HV-MV}}{Z_{11:j-k} + Z_{11:L_k}} - \frac{Z_{11:L_j}}{Z_{11:L_k}} \cdot \frac{Z_{11:HV-MV}}{Z_{11:j-k}}}{\frac{Z_{11:HV-j}}{Z_{11:L_j}} + \frac{Z_{11:HV-j}}{Z_{11:j-k} + Z_{11:L_k}}} \cdot VUF_{k:\text{net}}$	$\frac{Z_{11:j-k}}{Z_{11:HV-k}} \cdot VUF_{L_j}$ $+ \frac{Z_{11:HV-j}}{Z_{11:HV-k}} \cdot \frac{Z_{11:L_k}}{Z_{11:L_k} + Z_{11:j-k}} \cdot VUF_{k:\text{net}}$	$\frac{Z_{11:j-k} + Z_{11:L_k}}{Z_{11:HV-j}} VUF_{L_k}$ $+ \left( \frac{Z_{11:j-k} + Z_{11:L_k}}{Z_{11:L_k}} \right) \cdot VUF_{j:\text{net}}$

MV busbar  $VUF_{MV:\text{net}}$ , the total VUF at the  $j^{\text{th}}$  busbar  $VUF_{j:\text{net}}$  and the total VUF at the  $k^{\text{th}}$  busbar  $VUF_{k:\text{net}}$  respectively, when both loads are operating simultaneously.

In Table II,  $VUF_{L_j}$  is termed as the VU emission from the unbalanced installation connected to  $j^{\text{th}}$  busbar and is equal to the VUF at the  $j^{\text{th}}$ , when load  $L_j$  is operating in isolation. Similarly,  $VUF_{L_k}$  is termed as the VU emission from the unbalanced installation connected to  $k^{\text{th}}$  busbar and is equal to the VUF at the  $k^{\text{th}}$ , when load  $L_k$  is operating in isolation. Expressions for  $VUF_{L_j}$  and  $VUF_{L_k}$  are given in (13) and (14) respectively.

$$VUF_{L_j} = -\frac{Z_{11:HV-j}}{Z_{11:L_j}} \cdot CUF_{L_j} \quad (13)$$

$$VUF_{L_k} = -\frac{Z_{11:HV-k}}{Z_{11:L_k}} \cdot CUF_{L_k} \quad (14)$$

According to Table II, when both loads are operating simultaneously, VUFs at the  $j^{\text{th}}$  and  $k^{\text{th}}$  busbar can be expressed in-terms of the VUF caused by the load connected to the particular busbar and the VUF transferred to the busbar from upstream and/or downstream busbars (i.e. VUF of the adjacent busbars). Similarly, the VUF at the MV busbar can be expressed in-terms of the VUF propagated to the MV busbar from both the  $j^{\text{th}}$  and  $k^{\text{th}}$  busbars. Furthermore, referring to (13), (14) and Table II indicate that VU emission from the load connected to a particular busbar and VU propagation have been affected when both loads are operating simultaneously, compared to the situation in which individual loads are operating in isolation. Similar expressions can be developed for the VUF for each busbar when multiple numbers of loads are connected to the network. However, the complexity of such expressions will significantly increase; hence, the evaluation of the VU emission and propagation using a deterministic approach would be difficult.

## V. ESTIMATION OF VOLTAGE UNBALANCE AT VARIOUS LOCATIONS OF A RADIAL FEEDER

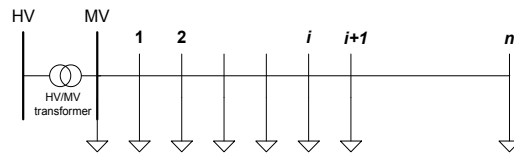


Fig. 3. Radial distribution network with multiple installations

$$(VUF_{i:\text{net}})^\alpha = (VUF_{L_{\text{MV}}})^\alpha + \sum_{m=1}^i [VUF_{L_m}]^\alpha + \sum_{m=i+1}^n \left[ \frac{S_{sc:i}}{S_{sc:m}} VUF_{L_m} \right]^\alpha \quad (15)$$

$$(VUF_{\text{MV}:\text{net}})^\alpha = (VUF_{L_{\text{MV}}})^\alpha + \sum_{m=1}^n \left[ \frac{S_{sc:\text{MV}}}{S_{sc:m}} VUF_{L_m} \right]^\alpha \quad (16)$$

$$(VUF_{n:\text{net}})^\alpha = (VUF_{L_{\text{MV}}})^\alpha + \sum_{m=1}^n [VUF_{L_m}]^\alpha \quad (17)$$

As demonstrated in Section IV, when multiple unbalanced installations are operating simultaneously, the VU emission of each unbalanced installation can be influenced by the other unbalanced installations connected to adjacent busbars. Consequently, the development of a deterministic approach to estimate the net VU at each busbar would be difficult. A general summation law based on a statistical approach is proposed in [4] as a means for calculation of disturbances caused by multiple sources.

In order to establish a general expression for VUF at various locations along a feeder where multiple unbalanced installations are connected, consider the radial distribution network given in Fig. 3. The voltage at the upstream HV busbar is considered to be balanced. Multiple unbalanced installations are connected to the MV busbar and intermediate busbars 1 to  $n$ . The distribution line sections are assumed to be symmetrical. Considering one installation at a time, when VU propagates upstream of the point of connection of the installation under consideration, it can be expressed in terms of VU transfer coefficient. Referring to Section II the VU transfer coefficient from downstream to upstream of the network can be approximated by the ratio of fault levels of two locations and VU transfer coefficient from the PCC of the installation to a downstream point of the network will be equal to unity as there are no further installations connected at downstream.

Following the aforementioned principles and summation law proposed in [4], a general expression for VUF at the  $i^{\text{th}}$  busbar can be formulated. The net VUF at the  $i^{\text{th}}$  busbar results from the VU that propagates to the  $i^{\text{th}}$  busbar from all other unbalanced installations connected upstream of the  $i^{\text{th}}$  busbar (including the installations connected to the MV busbar), the VU emission from the installation connected at the  $i^{\text{th}}$  busbar and the VU that propagates to the  $i^{\text{th}}$  busbar from all other unbalanced installations located downstream of the  $i^{\text{th}}$  busbar. Hence, the VUF at the  $i^{\text{th}}$  busbar ( $VUF_{i:\text{net}}$ ) can be written as (15). Similarly, the VUF at the MV busbar ( $VUF_{\text{MV}:\text{net}}$ ) and VUF at the  $n^{\text{th}}$  busbar ( $VUF_{n:\text{net}}$ ) can be given by (16) and (17) respectively. In (15)–(17), the following terms are defined;

- $VUF_{\text{MV}:\text{net}}$  the resultant VUF at MV busbar
- $VUF_{L_{\text{MV}}}$  is the magnitude of the VUF caused by the unbalanced installations directly connected to the MV busbar or VUF that propagates to the MV busbar in the case where there are parallel feeders
- $VUF_{L_m}$  is the magnitude of the VUF caused by the unbalanced installations connected to downstream of the MV busbar as evaluated by (18)<sup>5</sup>,

$$VUF_{L_m} \approx \frac{S_{sc:m}}{S_m} \cdot CUF_{L_m} \quad (18)$$

- $S_{sc:m}$  is the fault level at any intermediate busbar  $m$

<sup>5</sup>Referring to (13),  $VUF_{L_m}$  can be written as  $VUF_{L_m} = -\frac{Z_{11:\text{HV}-m}}{Z_{11:L_m}} \cdot CUF_{L_m}$ . Hence,  $|VUF_{L_m}| = \left| -\frac{Z_{11:\text{HV}-m}}{Z_{11:L_m}} \right| \cdot |CUF_{L_m}|$ . Considering that  $S_{sc:m} = \left| \frac{V_n}{Z_{11:\text{HV}-m}} \right|$  and  $S_m \approx \left| \frac{V_n}{Z_{11:L_m}} \right|$ ,  $|VUF_{L_m}|$  can be written as (18).

- $S_m$  is the MVA capacity of the load
- $CUF_{L_m}$  is the CUF of the load connected to the  $m^{\text{th}}$  busbar, which can be evaluated by either through a load flow analysis or by measurement<sup>6</sup>.
- $S_{sc:MV}$  is the fault level at the MV busbar

With reference to (15)-(17), the equations provide a significantly simpler methodology, where the VU in a radial distribution network can be estimated using readily available data such as the MVA capacity of all distribution loads, fault levels at the POE of each load and so forth.

## VI. IMPACT OF INDUCTION MOTORS ON VOLTAGE UNBALANCE EMISSION AND ATTENUATION

Three-phase induction motors connected to distribution networks are known to attenuate VU and hence impact on VU emission and propagation in the network. Considering the radial distribution network in Fig.1, the impact of induction motors on VU attenuation and propagation is examined in this section. The following three scenarios are considered.

**Scenario I:** In the distribution network given in Fig. 1, an unbalanced passive load and an induction motor are connected to the  $j^{\text{th}}$  and  $k^{\text{th}}$  busbars respectively. The VU emission from the load connected to the  $j^{\text{th}}$  busbar,  $VUF_{L_j}$  (which is same as  $VUF_j$ ) and the VUF at the MV busbar are given by (19) and (21) respectively.

$$VUF_{L_j} = K_1 \cdot \frac{Z_{11:HV-j}}{Z_{11:L_j}} \cdot CUF_{L_j} \quad (19)$$

where,

$$K_1 = \frac{Z_{22:j-k} + Z_{22:m_k}}{Z_{22:HV-k} + Z_{22:m_k}} \quad (20)$$

$$VUF_{MV} = \frac{\left( \frac{(1-K_2) \cdot Z_{11:MV-j} - K_2 \cdot Z_{11:HV-MV}}{Z_{11:L_j}} \right)}{\frac{Z_{11:MV-j} + Z_{11:L_j}}{Z_{11:L_j}} + \frac{Z_{11:MV-j}}{Z_{22:j-k} + Z_{22:m_k}}} \cdot CUF_{L_j} \quad (21)$$

where,

$$K_2 = \frac{Z_{22:MV-k} + Z_{22:m_k}}{Z_{22:HV-k} + Z_{22:m_k}} \quad (22)$$

where;  $Z_{11:m_k}$ ,  $Z_{22:m_k}$  positive-sequence and negative-sequence impedances<sup>7</sup> of the induction motor connected to the  $k^{\text{th}}$  busbar respectively.

**Scenario II:** The distribution network is modified by placing the induction motor at the  $j^{\text{th}}$  busbar and the unbalanced load at the  $k^{\text{th}}$  busbar in the network given in Fig. 1. The resulting expressions for The VUF at the PCC of the load connected to the  $k^{\text{th}}$  busbar  $VUF_{L_k}$  (which is same as  $VUF_k$ ) and VUF at the MV busbar are given by (23) and (25) respectively.

$$VUF_{L_k} = \frac{K_3 \cdot (Z_{11:HV-j}) + Z_{11:j-k}}{Z_{11:L_k}} \cdot CUF_{L_k} \quad (23)$$

where;

<sup>6</sup>CUF of the load connected to the  $m^{\text{th}}$  busbar  $CUF_{L_m}$  is different when multiple loads are operating simultaneously, compared to the situation where load connected to the  $m^{\text{th}}$  busbar is operating in isolation. However, such discrepancy are minor and can be shown to be negligible through numerical examples.

<sup>7</sup>In contrast to a passive load, the negative-sequence impedance of an induction motor is different to its positive-sequence impedance

$$K_3 = \frac{Z_{22:m_j}}{Z_{22:HV-j} + Z_{22:m_j}} \quad (24)$$

$$VUF_{MV} = \frac{\left( \frac{(1-K_4) \cdot Z_{11:MV-j} - K_4 \cdot Z_{11:HV-MV}}{Z_{11:j-k} + Z_{11:L_k}} \right)}{\frac{Z_{11:MV-j} + Z_{11:m}}{Z_{11:m}} + \frac{Z_{11:MV-j}}{Z_{22:j-k} + Z_{22:L_k}}} \cdot CUF_{L_k} \quad (25)$$

where;

$$K_4 = \frac{Z_{22:MV-j} + Z_{22:m_j}}{Z_{22:HV-j} + Z_{22:m_j}} \quad (26)$$

**Scenario III:** The VUFs at the PCC of the unbalanced load and VUF at the MV busbar when the induction motor and the unbalanced load are placed in two parallel feeders as shown in Fig. 4 are given by (27) and (28) respectively. Note that the  $j^{\text{th}}$  and  $k^{\text{th}}$  busbars are now connected to two parallel feeders.

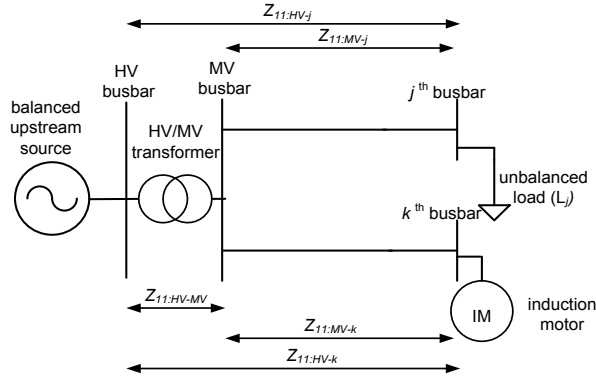


Fig. 4. Induction motor load and an unbalanced passive load connected to two parallel feeders.

$$VUF_{L_j} = \frac{K_5 \cdot Z_{11:HV-MV} + Z_{11:MV-j}}{Z_{11:L_j}} \cdot CUF_{L_j} \quad (27)$$

$$VUF_{MV} = \left( \frac{K_5 \cdot Z_{11:HV-MV}}{Z_{11:L_j}} \cdot CUF_{L_j} \right) \cdot \frac{Z_{11:L_j}}{Z_{11:L_j} + Z_{11:MV-j}} \quad (28)$$

where;

$$K_5 = \frac{Z_{22:MV-k} + Z_{22:m_k}}{Z_{22:HV-k} + Z_{22:m_k}} \quad (29)$$

Note that the magnitudes of the factors  $K_1$ ,  $K_3$  and  $K_5$  are less than unity. Therefore, referring to (7), (19), (23), (27) and assuming that the CUF of the passive load does not substantially change, the VUF at PCC of the load can be observed to decrease when induction motor loads are connected in the proximity of the load.

In order to verify (19), (23) and (27), four cases were considered.

- Case 1: Only an unbalanced load is connected to the  $j^{\text{th}}$  busbar of the MV distribution network discussed in Section III (refer to Fig. 1), and length of the distribution line between MV busbar and  $j^{\text{th}}$  busbar,  $l_{MV-j} = 0.8$  km.
- Case 2: An unbalanced load and an induction motor load are connected to the  $j^{\text{th}}$  and  $k^{\text{th}}$  busbars of the MV distribution network discussed in Section III respectively, and  $l_{MV-j} = 0.8$  km and  $l_{j-k} = 0.4$  km

- Case 3: An induction motor and an unbalanced load are connected to the  $j^{\text{th}}$  and  $k^{\text{th}}$  busbars of the MV distribution network discussed in Section III respectively, and  $l_{MV-j} = 0.4$  km and  $l_{MV-k} = 0.8$  km
- Case 4: An unbalanced load and an induction motor load are connected to  $j^{\text{th}}$  and  $k^{\text{th}}$  busbars respectively in two parallel feeders in the distribution network given in Fig. 4, and  $l_{MV-j} = 0.8$  km and  $l_{MV-k} = 0.4$  km

The unbalanced loads have per-phase MVA capacity of 4 MVA with lagging power factors of 0.6, 0.7 and 0.8 in phases A, B and C respectively. A 2.3 kV, 2250 hp induction motor which is connected to the distribution network through a 12.4/2.3 kV motor servicing transformer is considered. The impedance of the motor servicing transformer and equivalent circuit parameters of the induction motor are given in Appendix B. The comparison of results for VUF at the MV busbar, VUF at PCC of the unbalanced load ( $VUF_L$ ) and VU transfer coefficient from load busbar to MV busbar ( $T_{u:L-MV}$ ), obtained from the mathematical models in (19)-(29) and load-flow analysis using DIgSILENT PowerFactory software are given in Table. III. The resulting complex CUF of the passive loads are shown in Fig. 5. According to the results tabulated in Table III, the VU emission from the unbalanced loads have reduced when an induction motor load is connected to the network. However, the VU transfer coefficient,  $T_{u:L-MV}$ , has remained approximately constant irrespective of the presence of induction motor load. Furthermore, according to Fig. 5, the complex CUFs of the passive load shows only a negligible difference for all four cases considered in the study.

TABLE III  
COMPARISON OF RESULTS FOR  $VUF_{MV}$ ,  $VUF_L$  AND  $T_{u:L-MV}$ .

Case	$VUF_{MV}$		$VUF_L$		$T_{u:L-MV}$	
	load-flow analysis	mathematical formulation	load-flow analysis	mathematical formulation	load-flow analysis	mathematical formulation
1	0.43∠2.83	0.44∠2.83	0.63∠2.71	0.64∠2.71	0.68	0.68
2	0.40∠2.84	0.41∠2.83	0.59∠2.72	0.60∠2.72	0.67	0.68
3	0.40∠2.83	0.41∠2.83	0.60∠2.71	0.60∠2.72	0.67	0.68
4	0.41∠2.83	0.42∠2.83	0.61∠2.71	0.62∠2.71	0.67	0.67

Fig. 6 illustrates the variation of the VUF at the PCC of the unbalanced load when the position of the induction motor load is varied along the the feeder, when the unbalanced load is connected at 0.8 km away from the MV busbar and (a) the induction motor load are connected at the same feeder, (b) the induction motor load are connected to a parallel feeder. According to Fig. 6, the VUF at the PCC of the load has reduced to 0.61% from 0.63% when the induction motor is connected to a parallel feeder, but remains constant irrespective of the point of connection in the parallel feeder. When the induction motor is connected to the same feeder as the unbalanced load, the VU emission from the load further decreases from 0.61% when the PCC of the induction motor load is moved from the MV busbar towards the PCC of the unbalanced load. The minimum value can be observed when the PCC of the load and the PCC of induction motor load coincide with each other. When the PCC of the induction motor load is moved further away from the passive load, the VU emission from

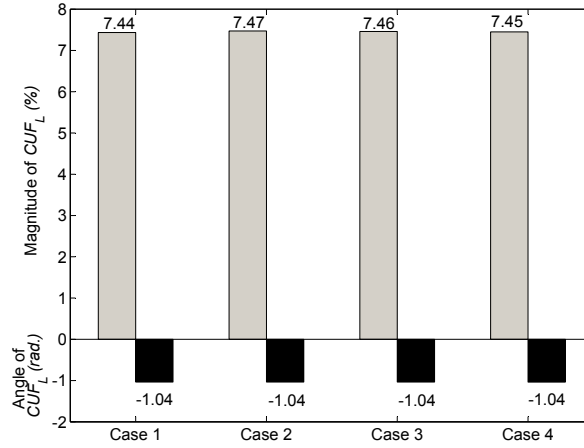


Fig. 5. Variation of CUF of the unbalanced load for cases 1-4.

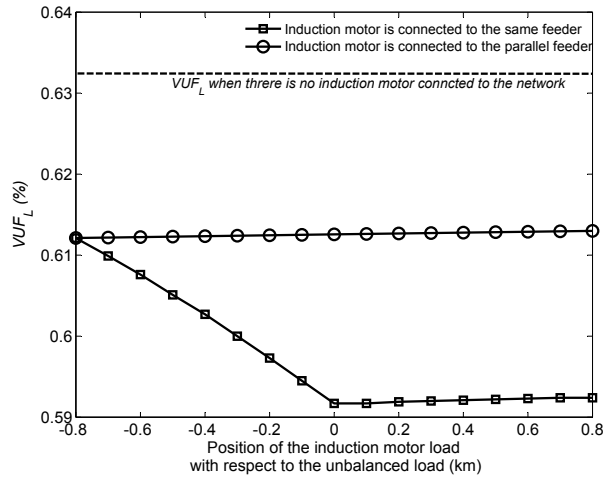


Fig. 6. Variation of VU emission with the position<sup>8</sup> of the induction motor.

TABLE IV  
INFLUENCE COEFFICIENTS

<b>Scenario I</b> (Unbalanced passive load and an induction motor are connected to $j^{\text{th}}$ busbar and $k^{\text{th}}$ busbar respectively)	$\beta = \frac{Z_{22:j-k} + Z_{22:m}}{Z_{22:HV-k} + Z_{22:m}}$
<b>Scenario II</b> (Induction motor and an unbalanced passive load are connected to $j^{\text{th}}$ busbar and $k^{\text{th}}$ busbar respectively)	$\beta = \frac{K \cdot (Z_{11:HV-j}) + Z_{11:j-k}}{Z_{11:HV-MV}}$ where $K = \frac{Z_{22:m}}{Z_{22:HV-j} + Z_{22:m}}$
<b>Scenario III</b> (Unbalanced passive load and an induction motor are connected to $j^{\text{th}}$ busbar and $k^{\text{th}}$ busbar in two parallel feeder as shown in Fig.4)	$\beta = \frac{K \cdot Z_{11:HV-MV} + Z_{11:MV-j}}{Z_{11:HV-j}}$ where $K = \frac{Z_{22:MV-k} + Z_{22:m}}{Z_{22:HV-k} + Z_{22:m}}$

the load shows a negligible increase.

An influence factor ( $\beta$ ) is defined by (30) to quantify the VU attenuation provided by the induction motor at the PCC of the unbalanced loads in a radial power system.

$$\beta = \frac{VUF_L \text{ with the induction motor load}}{VUF_L \text{ without induction motor load}} \quad (30)$$

Assuming that the change of the CUF of the unbalanced load is negligible when induction motor load is connected, the influence factor for scenarios I-III considered in this section are summarised in Table IV. A comparison of the influence factors evaluated using the formulations given in Table IV and load-flow analysis for cases 2-4 are given in Fig. 7. The magnitude of the influence factor estimated using the proposed formations in Table IV is in close agreement with the load-flow results.

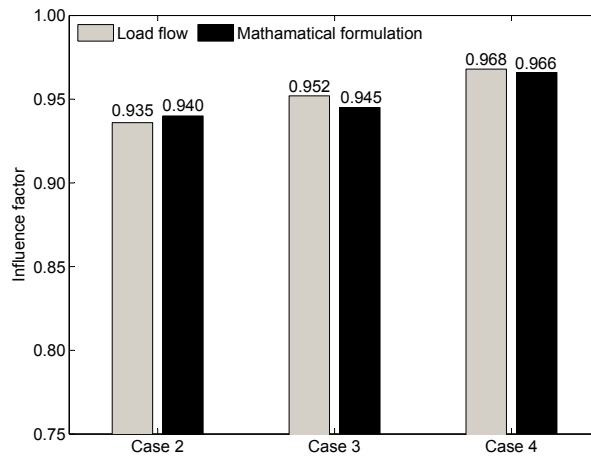


Fig. 7. Comparison of influence factors of mathematical formulation and load-flow analysis.

## VII. CONCLUSIONS

This paper has presented a detailed analysis of VU attenuation and propagation in radial distribution lines. Methodologies for estimating the VU transfer coefficients are developed where it is shown that the VU transfer coefficients from downstream to upstream network can be conservatively approximated using the ratio of fault levels between the two points. The VU propagation and attenuation, when multiple unbalanced loads are connected has also been discussed. A general approach for estimating the VU in a radial distribution network when multiple unbalanced loads are operating has been developed based on the general summation law. An influence factor has been derived to quantify the impact of induction motor to attenuate VU in radial distribution networks.

Based on the proposed methodologies to evaluate VU propagation and attenuation, the existing VU emission allocation methodologies in IEC 61000-3-13 can be further modified to allow higher emission limits for unbalanced loads connected to radial distribution networks.

<sup>8</sup>The distance is measured with respect to the position of the unbalanced load.

## LIST OF SYMBOLS

$Z_{11:HV-MV}, Z_{22:HV-MV}$	positive-sequence and negative-sequence impedance of the HV/MV transformer respectively
$Z_{11:MV-j}, Z_{22:MV-j}$	positive-sequence and negative-sequence impedance of the distribution line between the MV busbar and $j^{\text{th}}$ busbar respectively
$Z_{11:j-k}, Z_{22:j-k}$	positive-sequence and negative-sequence impedance of the distribution line between the $j^{\text{th}}$ busbar and $k^{\text{th}}$ busbar respectively
$Z_{11:HV-j}, Z_{22:HV-j}$	positive-sequence and negative-sequence impedance of the system between the HV busbar and $j^{\text{th}}$ busbar respectively
$Z_{11:HV-k}, Z_{22:HV-k}$	positive-sequence and negative-sequence impedance of the system between the HV busbar and $k^{\text{th}}$ busbar respectively
$Z_{21:HV-MV}$	negative-sequence positive-sequence coupling impedance
$Z_{21:HV-j}$	negative-sequence positive-sequence coupling impedance of the system between the HV busbar and the $j^{\text{th}}$ busbar
$U_{1:HV}, U_{2:HV}$	positive-sequence and negative-sequence voltages at the HV busbar respectively
$U_{1:MV}, U_{2:MV}$	positive-sequence and negative-sequence voltages at the MV busbar respectively
$U_{1:j}, U_{2:j}$	positive-sequence and negative-sequence voltages at the $j^{\text{th}}$ busbar respectively
$I_{1:L_j}$ and $I_{2:L_j}$	are positive-sequence and negative-sequence currents of the load which is connected at the $j^{\text{th}}$ busbar respectively
$CUF_{L_j}$	current unbalance factor (CUF) at the $j^{\text{th}}$ busbar
$Z_{11:L_j}$	positive-sequence impedance of the load connected at the $j^{\text{th}}$ busbar
$VUF_{MV}$	VUF at the MV busbar
$T_{u:j-MV}$	The VU transfer coefficient from the $j^{\text{th}}$ busbar to MV busbar
$S_{sc:MV}$	short-circuit capacity (in MVA) at the MV busbar,
$S_{sc:j}$	short-circuit capacity (in MVA) at the $j^{\text{th}}$ busbar
$V_n$	nominal line to line voltage of the network
$VUF_{MV:net}$	total VUF at the MV busbar
$VUF_{j:net}$	total VUF at the $j^{\text{th}}$ busbar
$VUF_{k:net}$	total VUF at the $k^{\text{th}}$ busbar
$Z_{11:m_k}$	positive-sequence impedance of the induction motor connected to the $k^{\text{th}}$ busbar
$Z_{22:m_k}$	negative-sequence impedances of the induction motor connected to the $k^{\text{th}}$ busbar
$Z_{10:HV-j}$	positive-sequence zero-sequence coupling impedance of the system between the HV busbar and $j^{\text{th}}$ busbar
$Z_{20:HV-j}$	negative-sequence zero-sequence coupling impedance of the system between the HV busbar and $j^{\text{th}}$ busbar
$Z_{12:HV-j}$	negative-sequence positive-sequence coupling impedance of the system between the HV busbar and $j^{\text{th}}$ busbar
$I_{0:L_j}$	zero-sequence current of the load

## APPENDIX A

## DERIVATION OF EQUATION (1)-(4)

For the radial distribution line given in Fig. 1, the positive-sequence and negative-sequence voltage at the HV busbar and  $j^{\text{th}}$  busbar are related as,



$$U_{1:HV} = Z_{10:HV-j} \cdot I_{0:L_j} + Z_{11:HV-j} \cdot I_{1:L_j} + Z_{12:HV-j} \cdot I_{2:L_j} + U_{1:j} \quad (\text{A.1})$$

$$U_{2:HV} = Z_{20:HV-j} \cdot I_{0:L_j} + Z_{21:HV-j} \cdot I_{1:L_j} + Z_{22:HV-j} \cdot I_{2:L_j} + U_{2:j} \quad (\text{A.2})$$

where;  $Z_{10:HV-j}$  - positive-sequence zero-sequence coupling impedance of the system between the HV busbar and  $j^{\text{th}}$  busbar,  $Z_{20:HV-j}$  - negative-sequence zero-sequence coupling impedance of the system between the HV busbar and  $j^{\text{th}}$  busbar,  $Z_{12:HV-j}$  - negative-sequence positive-sequence coupling impedance of the system between the HV busbar and  $j^{\text{th}}$  busbar, and  $I_{0:L_j}$  - zero-sequence current of the load. Other symbols have their usual meanings as defined in Section II.

In general  $Z_{10:HV-j}$  and  $Z_{20:HV-j}$  are relatively small and  $I_{0:L_j} = 0$ . Therefore the voltage drop terms  $Z_{10:HV-j} \cdot I_{0:L_j}$  and  $Z_{20:HV-j} \cdot I_{0:L_j}$  can be neglected in (A.1) and (A.2) [14]. Furthermore as  $I_{2:L_j}$  is relatively small compared to  $I_{1:L_j}$ , the voltage drop terms  $Z_{11:HV-j} \cdot I_{1:L_j} \gg Z_{12:HV-j} \cdot I_{2:L_j}$ . Hence,  $Z_{12:HV-j} \cdot I_{2:L_j}$  can be neglected in (A.1). Therefore (A.1) and (A.2) can be further simplified as given in (2) and (4). Similar relationships between the positive-sequence and negative-sequence voltages of HV busbar and MV busbar can be established and are given in (1) and (3).

## APPENDIX B NETWORK DATA

The network parameters of the HV/MV distribution network in Section III and Section VI.  
Line Parameters:

The phase impedance matrix ( $[Z_{abc}]/\text{km}$ ) of the 12.47 kV asymmetrical distribution line sections in Section II-B in  $\Omega/\text{km}$

$$\begin{bmatrix} 0.2494 + j0.8748 & 0.0592 + j0.4985 & 0.0592 + j0.4462 \\ 0.0592 + j0.4985 & 0.2494 + j0.8748 & 0.0592 + j0.4985 \\ 0.0592 + j0.4462 & 0.0592 + j0.4985 & 0.2494 + j0.8748 \end{bmatrix}$$

The phase impedance matrix ( $[Z_{abc}]/\text{km}$ ) of the 12.47 kV symmetrical distribution line sections in Section II-B in  $\Omega/\text{km}$

$$\begin{bmatrix} 0.2494 + j0.8748 & 0.0592 + j0.4811 & 0.0592 + j0.4811 \\ 0.0592 + j0.4811 & 0.2494 + j0.8748 & 0.0592 + j0.4811 \\ 0.0592 + j0.4811 & 0.0592 + j0.4811 & 0.2494 + j0.8748 \end{bmatrix}$$

Transformer parameters:

138/12.47 kV transformer: 20 MVA, 60 Hz, 0.0048+j0.09988 pu impedance

12.47/2.3 kV transformer: 5 MVA, 60 Hz, 0.01+j0.07937 pu impedance

Induction motor parameters [15]:

2.3 kV, 2250 hp, 60 Hz,  $r_s=0.0269 \Omega$ ,  $X_{ls}=0.226 \Omega$ ,  $X_M = 13.04 \Omega$ ,  $X'_{lr} = 0.226 \Omega$ ,  $R'_r = 0.022 \Omega$  and  $J = 63.87 \text{ kg.m}^2$

## REFERENCES

- [1] J. G. Mayordomo, L. F. Beites and J. L. Gutiérrez, "Assessment of Unbalance Emission Level Produced by Loads Using the Apparent Power Components," *European Transactions on Electrical Power*, 1996; **6**(6):381-381 DOI: 10.1002/etep.4450060603
- [2] R. S. Herrera and J. R. Vázquez, "Identification of unbalanced loads in electric power systems," *International transactions on electrical energy systems*, 2014, **24**:1232-1243 DOI: 10.1002/etep.1772
- [3] Z. Liu and J. V. Milanović, "Probabilistic Estimation of Voltage Unbalance in MV Distribution Networks With Unbalanced Load," *IEEE Transactions on Power Delivery* (Early Access), DOI: 10.1109/TPWRD.2014.2322391
- [4] "Electromagnetic compatibility (EMC) - limits - assessment of emission limits for the connection of unbalanced installations to MV, HV and EHV power systems," Technical Report IEC/TR 61000-3-13, Ed. 1, International Electrotechnical Commission, 2008.
- [5] T. E. Seiphetlo and A. P. J. Rens, "On the Assessment of Voltage Unbalance," in *14th Int. Conf. Harmonics and Quality of Power*, 2010, DOI: 10.1109/ICHQP.2010.5625366
- [6] P. Paranavithana, "Contributions Towards the Development of the Technical Report IEC/TR 61000-3-13 on Voltage Unbalance Allocation," Ph.D. Dissertation, School of Electrical, Computer and Telecommunications Engineering, University of Wollongong, Australia, March 2009.
- [7] M. Chindris, A. Cziker, A. Miron, H. Balan, A. Iacob and A. Sudria, "Propagation of Unbalance in Electric Power Systems," in *9th Int. Conf. Elect. Power Quality and Utilisation*, 9-11 Oct. 2007. DOI: 10.1109/EPQU.2007.4424221
- [8] P. Paranavithana, S. Perera and R. Koch, "An Improved Methodology for Determining MV to LV Voltage Unbalance Transfer Coefficient," in *13th Int. Conf. Harmonics and Quality of Power*, Sep 28–Oct. 1, 2008. DOI: 10.1109/ICHQP.2008.4668860
- [9] U. Jayatunga, S. Perera and P. Ciufu, "Voltage Unbalance Emission Assessment in Radial Power Systems," *IEEE Trans. on Power Delivery*, vol.27, no.3, pp.1653-1661, July 2012. DOI: 10.1109/TPWRD.2012.2196294
- [10] U. Jayatunga, S. Perera, P. Ciufu, "Impact of Mains Connected Three-Phase Induction Motor Loading Levels on Network Voltage Unbalance Attenuation," 2012 IEEE International Conference on Power System Technology (POWERCON), Oct. 30 - Nov. 2, 2012. DOI: 10.1109/PowerCon.2012.6401337
- [11] H. Renner, "Voltage Unbalance Emission Assessment," in *Proc. Elect. Power Quality Supply Reliability Conf.*, 2010, vol.16, no.18, pp.43-48, June 2010. DOI: 10.1109/PQ.2010.5550022
- [12] P.C. Anderson, "Analysis of Faulted Power Systems," Wiley-IEEE Press, 1995.
- [13] A. Von Jouanne and B. Banerjee, "Assessment of Voltage Unbalance," *IEEE Trans. Power Del.*, vol.16, no.4, pp.782-790, Oct 2001. DOI: 10.1109/61.956770
- [14] "Review of disturbance emission assessment techniques," CIGRE/CIGRE C4.109 WG Report 468, June 2011.
- [15] P. C. Krause, O. Wasynczuk and S. D. Sudhoff, "Analysis of Electric Machinery and Drive Systems," Second Ed., John Wiley and Sons Inc., pp. 165, 2002.